Journal of Medicinal Chemistry

Article

Discovery of LY3104607: A Potent and Selective G Protein-Coupled Receptor 40 (GPR40) Agonist with Optimized Pharmacokinetic Properties to Support Once Daily Oral Treatment in Patients with Type 2 Diabetes Mellitus

Chafiq Hamdouchi, Pranab Maiti, Alan M. Warshawsky, Amy C. DeBaillie, Keith A. Otto, Kelly L. Wilbur, Steven D. Kahl, Anjana Patel Lewis, Guemalli R. Cardona, Richard W. Zink, Keyue Chen, Siddaramaiah CR, Jayana P. Lineswala, Grace L. Neathery, Cecilia Bouaichi, Benjamin A. Diseroad,, Alison N Campbell, Stephanie A. Sweetana, Lisa A Adams, Over Cabrera, Xiaosu Ma, Nathan P. Yumibe, Chahrzad Montrose-Rafizadeh, Yanyun Chen, and Anne Reifel Miller

J. Med. Chem., **Just Accepted Manuscript** • DOI: 10.1021/acs.jmedchem.7b01411 • Publication Date (Web): 13 Dec 2017

ACS Publications

Journal of Medicinal Chemistry is published by the American Chemical Society. 1155 Sixteenth Street N.W., Washington, DC 20036

Discovery of LY3104607: A Potent and Selective G Protein-Coupled Receptor 40 (GPR40) Agonist with Optimized Pharmacokinetic Properties to Support Once Daily Oral Treatment in Patients with Type 2 Diabetes Mellitus

Chafiq Hamdouchi,*[,a] Pranab Maiti,[b] Alan M. Warshawsky,[a] Amy C. DeBaillie,[a] Keith A. Otto,[a] Kelly L. Wilbur,[a] Steven D. Kahl,[a] Anjana Patel Lewis,[a] Guemalli R. Cardona,[a] Richard W. Zink,[a] Keyue Chen,[a] Siddaramaiah CR,[b] Jayana P. Lineswala,[a] Grace L. Neathery,[a] Cecilia Bouaichi,[a] Benjamin A. Diseroad,[a] Alison N. Campbell,[a] Stephanie A. Sweetana,[a] Lisa A. Adams,[a] Over Cabrera,[a] Xiaosu Ma,[a] Nathan P. Yumibe,[a] Chahrzad Montrose-Rafizadeh,[a] Yanyun Chen,[a] Anne Reifel Miller[a]

[a]Lilly Research Laboratories, A division of Eli Lilly and Company, Lilly Corporate Center, DC: 0540, Indianapolis, IN 46285

[b]Jubilant Biosys Research Center, Bangalore, India

ABSTRACT:

Insert Abstract Figure here

As part of our program to identify potent GPR40 agonists capable of being dosed orally once daily in humans, we incorporated fused heterocycles into our recently disclosed spiropiperidine and tetrahydroquinoline acid derivatives **1**, **2** and **3** with the intention of lowering clearance and improving the maximum absorbable dose (Dabs). Hypothesis-driven structural modifications focused on moving away from the zwitterion-like structure and mitigating the N-dealkylation and O-dealkylation issues led to

triazolopyridine acid derivatives with unique pharmacology and superior pharmacokinetic properties. Compound **4** (LY3104607) demonstrated functional potency and glucose dependent insulin secretion (GDIS) in primary islets from rats. Potent, efficacious, and durable dose dependent reductions in glucose levels were seen during glucose tolerance test (GTT) studies. Low clearance and volume of distribution and high oral bioavailability were observed in all species. The combination of enhanced pharmacology and pharmacokinetic properties supported further development of this compound as a potential glucose-lowering drug candidate.

INTRODUCTION

Type 2 diabetes mellitus (T2DM) has become a serious global health care problem with an estimated 422 million adults living with diabetes worldwide in 2014, compared to 108 million in 1980[1]. While several oral treatments for T2DM are available, some are limited by undesired side effects such as hypoglycemia, liver damage, gastrointestinal symptoms, and weight gain. Therefore, alternative therapeutics with novel mechanisms are desired. The G protein-coupled receptor GPR40 is highly expressed in pancreatic β-cells. Upon binding endogenous medium and long chain unsaturated fatty acids, GPR40 promotes insulin secretion only when glucose levels are elevated[2-6]. By this glucose dependent insulin secretion (GDIS) mechanism, GPR40 offers an attractive target toward efficacious and safe T2DM therapies. Although the GPR40 mechanism of action is not completely understood, GPR40 has been reported to interact predominantly with the G protein α-subunit of the Gq family (Gαq).[7-9] In this signaling cascade, activation of Gαq protein-coupled receptors triggers an increase in phospholipase C (PLC) activity. Subsequent inositol 1,4,5-triphosphate (IP_3)-mediated intracellular calcium mobilization and protein kinase C (PKC) activation are linked to increased insulin secretion from pancreatic β-cells[10-13]. Thus, small molecule GPR40 agonists have been targeted to treat T2DM.[7-8] Synthetic GPR40 agonists have been reported to stimulate insulin secretion

in a glucose-dependent manner and to correct impaired glucose tolerance in rodents.[14-25] Recently, we reported the discovery and development of **1** (LY2881835), **2** (LY2922083) and **3** (LY2922470) as potent and selective GPR40 agonists. Compound **3** was taken into a 28-day multiple ascending dose **(**MAD) study in patients with T2DM. This clinical study provided proof of concept for **3** as a potential glucose-lowering therapy.[26] However, the duration of the pharmacodynamic (PD) effect of 3 did not allow for QD dosing. Toward this goal, subsequent discovery efforts focused on identifying compounds with lower predicted human clearance and higher fraction of dose absorbed. Metabolic pathways in hepatocytes were identified during our previous efforts; namely, oxidation at multiple sites, dealkylation (N and O), and conjugation (glucuronide and taurine). Therefore, hepatocyte clearance measurements were important to the design and prioritization of new compounds. Herein, we describe the identification of triazolopyridine acid derivatives as selective GPR40 agonists with unique pharmacology and superior pharmacokinetic (PK) properties relative to our previously developed compounds. Through optimization of key variables that influence free drug concentration after oral administration, such as fraction of dose absorbed and intrinsic clearance, compound **4** was identified as a suitable candidate for clinical study.

CHEMISTRY

The syntheses of [1,2,4]triazolo[1,5–a]pyridine acid derivatives are detailed in Schemes 1 and 2. Condensation of 6-aminopyridine-3-carboxylate **5** with ethyl N-(thioxomethylene)cabamate followed by cyclization in the presence of hydroxylamine hydrochloride yielded the 2-amino-[1,2,4]triazolo[1,5-a]pyridine **7** (Scheme 1). The amino group was converted into the bromide **8** using Sandmeyer reaction conditions. Reduction of the ester using excess DIBAL-H followed by treatment with thionyl chloride afforded chloride **9**. Reaction of [1,2,4]triazolo[1,5–a]pyridine **9** with (S)-ethyl 3-(4-hydroxyphenyl)hex-4-ynoate **10** in the presence of cesium carbonate afforded **11**. This bromide was coupled with boronic acids

under Suzuki-Miyaura conditions to give the corresponding esters **12a-c**. Hydrolysis of the esters **12a** and **12b** in the presence of potassium trimethylsilanoate or 5N NaOH afforded the final [1,2,4]triazolo[1,5–a]pyridine acid derivatives **13a** and **13b**. Alternatively, alkylation of the phenol **12c** under basic conditions using cesium carbonate followed by ester hydrolysis of the ester yielded carboxylic acids **15a-c**.

Insert Scheme 1 here

Compounds **4** and **27b** (Scheme 2) were synthesized by a slightly different route. Amino 2,4,6-trimethylbenzenesulfonate **19** was prepared by reaction of the oxime **16** with the arylsulfonyl chloride **17** and subsequent hydrolysis of oxime sulfonate **18** in the presence HClO4. Compound **19** was reacted with 6-aminopyridine-3-carboxylate to give diaminopyridin-l -ium-3-carboxylate-2,4,6-trimethylbenzenesulfonate **20**. Treatment with aldehydes **21a** and **21b** effected triazolo[1,5–a]pyridine ring formation yielding **22a** and **22b**, respectively. The phenol group of **22b** was alkylated under basic conditions to give methanesulfonyl-propoxy triazolopyridine **23b**. Reduction of esters **22a** and **23b** with excess DIBAL-H followed by reaction with PBr_3 yielded bromides **25a** and **25b**. Reaction of these bromides with (S)-ethyl 3-(4-hydroxyphenyl)hex-4-ynoate **10** in the presence of cesium carbonate afforded the corresponding coupling products **26a** and **26b**. Finally, ester hydrolysis in the presence of 5N NaOH afforded the desired [1,2,4]triazolo[1,5–a]pyridine acids **4** and **27b**.

Insert Scheme 2 here

This discovery chemistry route was acceptable to deliver gram quantities of **4.** Due to the safety concerns associated with compound **19**[27] an alternative approach was desired to provide kilogram quantities to support toxicological and clinical studies (Scheme 3). The process chemistry synthesis of **4** began with

compound **8**, which was prepared as described in Scheme 1 with optimization of reagent stoichiometry, solvent volumes, operating temperatures and reaction times. The bromide was coupled with (2,6-dimethylphenyl)magnesium bromide (**28**) under Negishi conditions to give ester **29**, which was reduced with DIBAL-H to yield alcohol **30**. Treatment of alcohol **30** with thionyl chloride provided chloride **31**. Reaction of **31** with (S)-ethyl-3-(4-hydroxyphenyl)hex-4-ynoate **10** in the presence of potassium carbonate afforded ethyl ester **26a**. Ester hydrolysis of **26a** in the presence of NaOH afforded **4**, which was recrystallized from ethanol and n-heptane to provide the desired polymorph of compound **4** in a 56% overall yield from compound **8** with 99.8% purity and 99.5% chiral purity. X-ray crystallography data confirmed the isomer was of the R configuration.

Insert Scheme 3 here

RESULTS AND DISCUSSION

Since GPR40 is a Gαq-coupled receptor, *in vitro* functional activity of our compounds was initially determined with a calcium flux primary assay using Fluorescence Imaging Plate Reader (FLIPR) technology. The calcium flux measurements were useful to characterize these new compounds as partial agonists with efficacies comparable to LY compounds **1-3**. However, these data did not correlate with subsequent *in vivo* activities.[26] Therefore, we examined the connection between *in vivo* results and data from a number of *in vitro* assays. The best *in vitro* to *in vivo* correlation was noted between β-arrestin signaling and glucose lowering, most likely driven by receptor binding kinetics and the equilibrium properties of the β -arrestin assay.[26] With a longer compound incubation time, this non-G-protein mediated signaling assay was used to drive structure activity relationship (SAR) efforts. Additionally, competitive radioligand binding assays confirmed that these compounds bind specifically to the allosteric 1 site like compounds **1-3**. Affinities (K_i)

of compounds in Tables 1were determined by measuring competitive inhibition of the tritiated Fasiglifam ([^{3}H]-TAK875) binding to membranes prepared from cells overexpressing recombinant human GPR40.[26]

In the current effort, we sought to improve the overall PK profiles of our potent GPR40 agonists primarily by minimizing the risk of O and N-dealkylation and by improving solubility. Having established the *S*-β-1-propynyl benzenepropanoic acid as an optimal headpiece in previous efforts by us[26] by us and others,[20, 23] we turned our attention toward variations to the central linker and the hydrophobic tail. A number of heterocycles were evaluated at the central linker region. Fused heterocycles such as 2-phenyl-[l,2,4]triazolo[1,5-a]pyridines proved to be the most interesting (Table 1). In the tail region, phenyls substituted with medium-sized lipophilic groups led to compounds with potent binding and functional activity, such as **4** with a 2,6-dimethyl phenyl group. The overall physicochemical properties of these ligands could be modulated effectively through modification of this tail group. Efforts to increase the polar surface area (PSA) to improve metabolism and solubility parameters resulted in **13a**, **15a**, **15b** and **7b** (tPSA = 101, 95, 106, and 129, respectively) with only slightly decreased β-arrestin activity.

Triazolopyridines with various substitutions at the 2 position showed good *in vitro* activity across species using human and rat GPR40 assays (Table 1). All GPR40 compounds tested in an equilibrium dialysis assay were highly protein bound in plasma (> 99%). However, no significant shift in potency was noted in a modified Ca^{2+} mobilization assay with 0.1% of serum albumin added. Since plasma protein binding (PPB) shifts in these *in vitro* assays did not predict the *in vivo* outcomes, SAR efforts did not try to increase free drug fraction (f_u). Instead, structural modifications focused on optimizing the key variables that influence free drug concentration after oral administration, namely fraction of dose absorbed and intrinsic clearance.[28] Finally, the incorporation of the triazolopyridine moiety into these compounds minimized the risk of PPAR cross-reactivity. Compounds in Table 1 demonstrated a lack of significant PPAR binding or

functional activity when tested at concentrations up to 30 μM. These compounds were also inactive in an adipogenesis assay in 3T3-L1 cells.

From this set of triazolopyridine-based GPR40 ligands, **4** emerged as a candidate for further characterization.

Insert Table 1 here

As shown in Table 3, **4** demonstrated significant improvement in physicochemical and biopharmaceutical properties relative to our previous compounds for development (**1**-**3**). Compound **4** showed good solubility in a DMSO/aqueous precipitation assay (last soluble concentration >100 μM, pH = 7.4) and the most stable developable form of the crystalline free acid anhydrate exhibited very good water solubility (0.173 mg/mL, pH = 8.1). Preclinical absorption modeling of rat and dog PK data supported a high effective permeability in humans (calculated human passive permeability, cPeff = 5.20 x 10^{-4} cm/sec). The maximum absorbable dose (Dabs, MiMBa modeling) for **4** of 593 mg in the fasted state and 919 mg in the fed state was calculated using measured solubility and calculated human passive permeability; these values were comparable to those for **3** and much higher than for **1** and **2**. Under controlled particle size, clinical absorption was predicted to be high (> 80% Fa) for doses up to ~350 mg.

From in vitro ADME studies, **4** showed minimal risk for potential drug-drug interactions mediated by CYP enzymes (IC_{50} values > 60 μM against human CYP isoforms 3A4, 2D6, 2C9). The in vitro metabolism of **4** was determined in rat, dog, and human cryopreserved hepatocytes. Plasma, urine, and bile samples from rats and plasma and urine samples from dogs were used to characterize the in vivo metabolism of **4**. Overall, the in vitro data predicted the major metabolic pathways observed in vivo. Compound **4** was metabolized by both CYP and non-CYP metabolic processes in all species. In rat, oxidation to metabolite **A** was the

prominent metabolic pathway, while in dog, direct glucuronide conjugation to form metabolite **B** predominated (Figure 1). From human recombinant CYP phenotyping studies, the predominant metabolizing CYP isoform was found to be CYP3A4 with minor involvement of CYP2J2. These data demonstrated significant optimization in the metabolism of **4** compared to **1**-**3**, which suffered from extensive O/N-dealkylation and from oxidation at multiple sites. The [1,2,4]triazolo[1,5–a]pyridine linker in **4** lacks the aromaticity believed to be responsible for benzylic oxidation and subsequent O-dealkylation. As shown in Table 3, the human microsomal metabolic stability of **4** improved dramatically from our previous compounds (5% metabolized for compound **4** vs 38, 44, and 24% for **1**-**3**). Human microsomal and hepatocyte intrinsic clearances were also dramatically lower for compound **4** (<0.0009 and 0.099 mL/min/kg, respectively). These in vitro ADME data translated into a significant improvement in total clearances in preclinical animal models and consequently into a much lower predicted human clearance (*vida infra*).

Insert Figure 1 here

Pharmacokinetic studies with **4** in Beagle dogs and Sprague Dawley rats are summarized in Table 2. Compound **4** displayed low total clearances and low volumes of distribution in both species. Following oral administration to fasted rats and dogs at doses of 1 and 3 mg/kg, respectively, **4** was rapidly absorbed (Tmax < 1 hr) and showed high oral bioavailabilities, 93% (rats) and 83% (dogs). At higher oral doses, absorption appeared to be delayed and less than proportional increases in exposure were observed from 10 to 500 mg/kg in rats and from 30 to 300 mg/kg in dogs.

Insert Table 2 here

Compound **4** had remarkably lower clearances (3 to17-fold) in preclinical species compared to our previous clinical candidates **1, 2**, and **3** (Table 3). These significantly lower clearances were anticipated from the higher metabolic stability of **4** across species and its improved physical properties. Introduction of triazolopyridine linker fixed the O and N-dealkylation, reduced the zwitterionic character, and increased the polar surface area of our previous spiropiperidine-based candidates **1-3**.

The PK data predicted **4** to have more sustained pharmacodynamic effect than **3**. Human clearance (CL) and volume of distribution (Vd) parameters were projected using the allometric scaling method. The projected human clearance of 1 L/hr for **4** was substantially lower than the observed human clearance of 11-14 L/hr for **3**. The human PK profiles of **4** and **3** were simulated using projected PK parameters for **4** and measured PK parameters from the SAD study for **3**. Through this simulation, **4** is expected to show a smaller peak-to-trough ratio than **3** (Figure 2 and Table 3). While no significant compound accumulation was observed in the clinical study with **3**, approximately 50% accumulation is predicted for **4** to provide better coverage during later part of the day with QD dosing.

Insert Figure 2 here

As part of our optimization and selection process for the identification of preferred (potential) clinical candidates, enhanced pharmacology and prolonged durability were key criteria. We examined the ability of **4** to induce insulin secretion in rat islets and provide durable glucose control during a chronic study in a rat disease model. The target selectivity of **4** was assessed against over 100 different GPCRs, kinases, enzymes and nuclear receptors and showed minimal activity (<50%) at 10 μM concentration; no activity was noted against the hERG channel at 100 μM.

Because activation of GPR40 is known to result in glucose dependent insulin secretion, primary islet assays were developed to characterize compounds that increase intracellular calcium in the GPR40 primary assays. While **4** did not enhance insulin secretion from primary rodent islets incubated in 2.8 mM glucose (data not shown), significant increases in insulin secretion were produced by primary rat islets using static culture conditions in 11.2 mM glucose (Figure 3).

Insert Figure 3 here

Oral glucose tolerance tests (OGTTs) in a rodent model of insulin resistance were used to assess the pharmacodynamics effects (potency, efficacy, and durability) of our GPR40 agonists in male Zucker fa/fa rats (10 weeks of age), glucose tolerances following an oral glucose challenge were determined 1 day and 21 days after daily oral administration of **4** or positive control compound **1** (Figure 4). On days 1 and 21, the area under the curves (AUCs) for glucose lowering were statistically significant for all doses of **4** tested (1, 3, and 10 mg/kg) and for the positive control. Weight and food consumption were not altered by any treatment during the study (data not shown). The similar glucose lowering ED_{90} values for 4 on day 1 (4.1 mg/kg) and on day 21 (5.0 mg/kg) suggest that GPR40 is not desensitized by **4** after 21 days of oral administration.

Insert Figure 4 here

In these preclinical pharmacology studies, **4** demonstrated the robust potency, efficacy, durability and selectivity to justify clinical testing. GDIS was shown in primary rat islets confirming the GPR40 agonist mechanism of **4**. Potent glucose lowering plus the lack of hypoglycemia during glucose tolerance tests in rodents after chronic dosing reflect the efficacy, durability, and safety of this compound. Compound **4**

demonstrated an *in vivo* pharmacology similar to compound **3** (glucose lowering in Zucker fa/fa rats on day 21: ED_{90} = 5.0 mg/kg for **4** and 3.3 mg/kg for **3**). The human efficacious dose of 88 mg [90% PI, 39-138] once daily for **4** was projected busing Zucker fa/fa rats efficacious exposure ($EAUC_{90}$), allometrically-projected human clearance, and the projected bioavailability.

Insert Table 3 here

CONCLUSION

Through the GDIS mechanism GPR40 activation provides an excellent approach for developing effective and safe therapies for the treatment of T2DM. Herein we have described our efforts culminating in the identification of a potent GPR40 agonist suitable for once daily oral treatment in humans. Our hypothesis-driven structural modifications focused on mitigating N-dealkylation and O-delakylation issues and on moving away from zwitterion-like structures. We identified triazolopyridine-carboxylic acid derivatives as GPR40 agonists with unique pharmacology, selectivity, and superior PK properties. Compound **4** emerged as the leading molecule through optimization of key variables that influence free drug concentration after oral administration; namely, fraction of dose absorbed and intrinsic clearance. Compound **4** demonstrated acceptable potency and efficacy in G protein- and β-arrestin-mediated signaling assays and GDIS in primary islets from rats. Potent, efficacious, and durable dose-dependent reductions in glucose levels were seen during glucose tolerance test (GTT) studies in insulin-resistant rats. In addition, high oral bioavailability along with low clearance and volume of distribution were observed in all species. Compound **4** was predicted to have an acceptable projected human efficacious dose and sustained exposure to support once daily oral treatment in humans based on preclinical data. Therefore, on the basis of its excellent *in vitro,*

ex vivo, and *in vivo* pharmacology and pharmacokinetic profile, **4** was advanced as a clinical candidate for the treatment of T2DM.

EXPERIMENTAL SECTION

Chemistry. Unless otherwise noted, all materials were obtained from commercial suppliers and used as obtained. Organic solvents were also purchased from commercial sources on scale, without additional purification. Reactions were monitored using Agilent 1100 or 1200 Series LCMS with ultraviolet light (UV) detection at 215 and 254 nm and a low resolution electrospray mode (ESI). HRMS data were recorded on an Agilent LC-MS TOF (time-of-flight), Model G1969A instrument. Purity was measured using Agilent 1100 or 1200 Series high performance liquid chromatography (HPLC) with UV detection at 215, 254, and 280 nm (15 min; 1.5 mL/min flow rate), eluting with a binary solvent system A and B using a gradient elution (A, water with 0.1% TFA; B, MeCN with 0.1% TFA). Unless otherwise noted, the purity of all compounds was ≥98%. Enantiomeric excess for compounds bearing a stereogenic center were determined using analytical HPLC. ^{1}HNMR spectra were recorded on a Bruker AV-400 (400 MHz) spectrometer at ambient temperature. Chemical shifts are reported in parts per million (δ) and are calibrated using residual signal from undeuterated solvent as an internal reference. Data for 1H NMR spectra are reported as follows: chemical shift (δ ppm) (multiplicity, coupling constant (Hz), integration). Multiplicities are reported as follows: s = singlet, d = doublet, t = triplet, q = quartet, m = multiplet, br = broad, or combinations thereof. Differential scanning calorimetry (DSC) was performed on a TA Instruments Q100 calorimeter in an aluminum Tzero pan under dry N_2 flowing at 50 mL/min.

We previously reported a patent application that described the discovery route to the synthesis and characterization of all the compounds that we report in this manuscript (**4**, **13a**, **13b**, **15a**, **15b**, **15c** and **27b**).[29] Herein we describe our process and development route to prepare the clinical candidate **4** in

kilogram quantities. The process for the preparation of **4** required modifications of the discovery synthesis to make the route scalable.

Process synthesis of [1,2,4]triazolo[1,5–a]pyridine acid 4

Methyl 6-(ethoxycarbonylcarbamothioylamino)pyridine-3-carboxylate (6). To a solution of methyl 6-aminopyridine-3-carboxylate (24.3kg, 160.1 mol) in THF (242 L) was added ethyl N-(thioxomethylene)carbamate (25.6 kg, 195.2 mol, 1.2 equiv). The reaction was heated to 45 to 50 °C and stirred for 15 hr. The reaction was cooled to 20 to 30 °C, concentrated, and solvent exchanged into MTBE. The resulting solids were filtered, rinsed with MTBE (39 L), and dried at 40 to 50 °C to provide the title compound as a yellow solid (41.4 kg, 91%). MS (ES+) $[M + H]^+$: calcd, 283.1; found, 283.2. ^{1}H NMR (400 MHz, DMSO, δ): 12.4 (bs, 1H), 12.0(bs, 1H), 8.9(d, J= 2.4 Hz, 1H), 8.75 (b, 1H), 8.38 (d, J= 2.4, 8.8 Hz, 1H), 4.24 (q, J= 7.1 Hz, 2H), 3.88 (s, 3H), 1.28 (t, J= 7.1 Hz, 3H).

Methyl 2-amino-[l,2,4]triazolo[l,5-a]pyridine-6-carboxylate (7). To a 40 to 45 °C solution of Hydroxylamine hydrochloride (16.6 kg , 238.9 mol, 1.6 equiv) and methyl 2-amino-[1,2,4]triazolo[1,5-a]pyridine-6-carboxylate (41.4 kg, 146.5 mol) in ethanol (827 L) was added diisopropylethylamine (38.8 kg, 300 mol, 2.05 equiv). The reaction was warmed to 55 to 60 °C and stirred for 8 hr. The reaction was cooled to 30 to 40 °C and concentrated. The resulting solid was filtered and slurried in water (216 L) at 20 to 30 °C for 3 hr. The solids were filtered and dried at 45 to 55 °C to provide the title compound as a white solid (26.8 kg, 96%). MS (ES^+) $[M + H]^+$: calcd, 192.1; found, 192.2.^{1}H NMR (400 MHz, DMSO, δ): 9.02 (d, J = 1.0 Hz, 1H), 7.85 (dd, J = 1.7, 9.2 Hz, 1H), 7.41 (d, J = 9.3 Hz, 1H), 6.38 (s, 2H), 3.87 (s, 3H).

Methyl 2-bromo-[1,2,4]triazolo [1,5 -a]pyridine-6-carboxylate (8). To a stirred solution of cupric bromide (60.0 kg, 280 mol, 1.9 equiv) in acetonitrile (267 L) was added /tert-butyl nitrite (27.1 kg, 280 mol, 1.9 equiv). The reaction mixture was heated to 45 to 55 °C. Methyl 2-amino-[l,2,4]triazolo[l,5-a]pyridine-6-carboxylate (26.8 kg, 140 mol) was added portion wise and the reaction mixture was heated at 45 to 55 °C for 2 hr. The reaction mixture was cooled to 20 to 30 °C and quenched with water (605 L). The resulting suspension was filtered through celite (5kg) and the layers were separated. The organic layer was washed with water (214 L), concentrated and solvent exchanged into ethyl acetate. n-Heptane (302 L) was added dropwise and the resulting solids were filtered, washed with n-Heptane (48 L) and slurried with celite (4 kg) and DCM (537 L) at 20 to 30 °C for 30 min. The suspension was filtered over silica gel (28 kg) and the filtrate was concentrated and then diluted with EtOAc (296 L). The EtOAc solution was concentrated and n-heptane (315 L) was added dropwise. The resulting solids were filtered, washed with n-heptane (37 L) and dried at 50 to 55 °C to give the title compound as an off white solid (22.6 kg, 63%). LCMS m/z $[M + H]^+$: calcd, 256.0; found, 256.0. 1H NMR (400 MHz, DMSO, δ): 9.49 (dd, J = 0.9, 1.6 Hz, 1H), 8.13 (dd, J = 1.7, 9.4 Hz, 1H), 7.92 (dd, J = 0.8, 9.4 Hz, 1H), 3.93 (s, 3H).

Methyl 2-(2,6-dimethylphenyl)-[1,2,4]triazolo[1,5-a]pyridine-6-carboxylate (29). To an argon inerted mixture of methyl 2-bromo-[1,2,4]triazolo [1,5 -a]pyridine-6-carboxylate (39.0 kg, 152.3 mol) and zinc chloride (25.1 kg, 1.2 equiv) in THF (24 L) was added Pd $(Ph_3)_4$ (9.4 kg, 0.05 equiv). The mixture was heated to 50 to 55 °C. To the mixture was added a THF solution of (2,6-dimethylphenyl)magnesium bromide (**28**) (251 kg with 20.2% assay, 228.99 mol, 1.5 equiv). The mixture was stirred at 50 – 55 °C for 2 to 3 hr and then cooled to 20 to 30 °C. The reaction mixture was quenched with an aqueous 10% NH_4Cl solution (207 L). The mixture was solvent exchanged into MTBE and then filtered through celite (10 kg). The layers were separated, and the organic layer was washed with 10% NH_4Cl solution (234 L), concentrated and

solvent exchanged into DCM to provide the title compound as a solution in DCM that was used directly in the next step (513 kg, 7.9% assay). LCMS m/z $[M + H]^+$: calcd, 281.3; found, 281.0. ^{1}H NMR (400.13 MHz, DMSO, δ): 9.54 (s, 1H), 8.10 (dd, J = 1.7, 9.3 Hz, 1H), 7.98 (d, J = 9.4 Hz, 1H), 7.31 (t, J = 7.6 Hz, 1H), 7.19 (d, J = 7.6 Hz, 2H), 3.94 (s, 3H), 2.12 (s, 6H).

[2-(2,6-Dimethylphenyl)-[1,2,4]triazolo[1,5-a]pyridin-6-yl]methanol (30). To a -15 to -5 °C solution of methyl 2-(2,6-dimethylphenyl)-[1,2,4]triazolo[1,5-a]pyridine-6-carboxylate (513 kg as a 7.9% assay) in DCM was added DIBAL-H (1.5 M solution toluene, 194 kg, 366.68 mol, 2.4 equiv). The reaction mixture was warmed to -5 to 0 °C and stirred for 2 hr. To the reaction mixture was charged DCM (340 L) and water (13.9 L). The mixture was stirred for 15 – 30 min and then a 15% aqueous solution of NaOH (16 L) was added followed by additional water (33 L). The reaction mixture was warmed to 25 to 30 °C and was stirred for 2-3 hr. The mixture was filtered through celite (10 kg) and the cake was washed with DCM (302 L). The filtrate was concentrated and a 10% potassium sodium tartrate solution (420 L) was added. The layers were separated and the organic layer was washed 2x with 2N HCl (410 L and 200 L, respectively). The combined aqueous layers were treated with 20% aqueous sodium carbonate solution (448 L). The resulting solid was filtered, washed with water (40 L), and dried under vacuum at 45 to 50 °C to provide the title compound as a yellow solid (30.8 kg, 80% over two steps). LCMS m/z $[M + H]^+$: calcd, 253.3; found, 253.0. ^{1}H NMR (400.13 MHz, DMSO, δ): 8.85 (s, 1H), 7.85 (d, J = 9.2 Hz, 1H), 7.67 (dd, J = 1.4, 9.1 Hz, 1H), 7.29 (t, J = 7.6 Hz, 1H), 7.17 (d, J = 7.7 Hz, 2H), 5.57-5.48 (m, 1H), 4.62 (s, 2H), 2.10 (s, 6H).

6-(Chloromethyl)-2-(2,6-dimethylphenyl)-[1,2,4]triazolo[1,5-a]pyridine (31). To a -5 to 0 °C solution of thionyl chloride (33.0kg, 277.4 mol, 2.3 equiv) in THF (167 L) was added *[2-(2,6-dimethylphenyl)-[1,2,4]triazolo[1,5-a]pyridin-6-yl]methanol* (30.6 kg, 121.0 mol) in THF (326 L). The solution was warmed

to 20 to 30 °C and stirred for 2 hr. The reaction mixture was concentrated and solvent exchanged into n-Heptane. The solid was filtered, washed with n-heptane (47 L) and dried at 35 °C to yield the title compound. The title compound was slurried in water (297 L) at 20 -30 °C, filtered, washed with water (31 L), and dried at 35 to 45 °C to give the title compound as an off-white solid (29.1 kg, 88%). LCMS m/z $[M + H]^+$: calcd, 271.7; found, 271.1. ^{1}H NMR (400.13 MHz, DMSO, δ): 9.19 (s, 1H), 7.92 (d, J = 9.2 Hz, 1H), 7.78 (dd, J = 1.6, 9.2 Hz, 1H), 7.30 (t, J = 7.6 Hz, 1H), 7.17 (d, J = 7.6 Hz, 2H), 4.95 (s, 2H), 2.10 (s, 6H).

Ethyl (3 S)-3 -[4- [[2-(2,6-dimethylpheny 1)- [1,2,4]triazolo[1,5-a]pyridin-6-yl]methoxy]phenyl]hex-4-ynoate (26a). To a solution of (S)-ethyl 3-(4-hydroxyphenyl) hex-4-ynoate (29.0 kg, 106.78 mol) and 6-(Bromomethy1)-2-(2,6-dimethylphenyl)- [l,2,4]triazolo[l,5-a]pyridine (25.8 kg, 111.18 mol, 1.04 equiv) in DMF (167 L) was added potassium carbonate (29.8 kg, 215.94 mol, 2.02 equiv). The mixture was heated to 35 °C -45 °C and was stirred for 20 hr. The reaction mixture was cooled to 20 °C -25 °C and EtOAc (336 L) and water (502 L) was added. The layers were separated, and the organic layer was washed with water (170 L). The organic layer was concentrated and the solvent exchanged into ethanol to give the title compound as a solution in ethanol that was used directly in the next step. LCMS m/z $[M + H]^+$: calcd, 467.5; found, 467.2. ^{1}H NMR (399.45 MHz, $CDCl_3$, δ): 8.73 (d, J = 0.6 Hz, 1H), 7.89 (d, J = 9.1 Hz, 1H), 7.64 (dd, J = 1.7, 9.1 Hz, 1H), 7.34-7.31 (m, 2H), 7.27-7.23 (m, 1H), 7.11 (d, J = 7.5 Hz, 2H), 6.96-6.94 (m, 2H), 5.14 (s, 2H), 4.15-4.08 (m, 3H), 2.77-2.61 (m, 2H), 2.17 (s, 6H), 1.81 (d, J = 2.4 Hz, 3H), 1.20 (t, J = 7.1 Hz, 3H).

(3S)-3-[4-[[2-(2,6-Dimethylphenyl)-[l,2,4]triazolo[l,5-a]pyridin-6-yl]methoxy]phenyl]hex-4-ynoic acid (4). To a solution of ethyl (3S)-3-[4-[[2-(2,6-dimethylphenyl)-[l,2,4]triazolo[l,5-a]pyridin-6-yl]methoxy]phenyl]hex-4-ynoate (106.8 mol) in ethanol was added aqueous 10% NaOH (78 L, 195 mol,

1.83 equiv) drop wise at a rate to maintain the reaction temperature below 30 °C. The reaction mixture was stirred for 4 hr and then concentrated. Water (333 L) was added, and the reaction mixture was concentrated. MTBE (170 L) was charged, and the layers were separated. EtOAc (352 L) was charged to the aqueous layer and the pH was adjusted to 4-5 with 1M HCl (234 L) at 15 – 20 °C. The layers were separated and the combined organic layers were washed with water (164 L), filtered through a CUNO filter, and concentrated. The reaction mixture was heated to 70-80 °C until a clear solution was obtained and then cooled to 65-75 °C. n-Heptane (409 L) was charged dropwise to maintain an internal temperature of 65-75 °C, and then the solution was slowly cooled to 5 °C. The resulting solids were filtered and washed with n-Heptane (91 L) and dried under vacuum at 40-45 °C to yield the title compound (42.15 kg, 88% over two steps). To the title compound (40.0 kg, 89.46 mol) was added ethanol (247 L), and the slurry was heated to 60-65 °C until a clear solution was obtained. The resulting solution was cooled to 45-55 °C and compound **4** (0.217 kg) was added. The solution was slowly cooled to 20-25 C, and then n-Heptane (724 L) was added dropwise. The slurry was cooled to 5-10 °C and allowed to stir for 2-3 hr. The solids were filtered, washed with n-Heptane (118 L), and dried under vacuum at 45-50 °C to yield the title compound as white solid (35.76 kg, 91%). LCMS m/z $[M + H]^+$: calcd, 439.5; found, 439.2. ^{1}H NMR (399.80 MHz, DMSO, δ): 12.22 (s, 1H), 9.13 (dd, J = 0.8, 1.5 Hz, 1H), 7.88 (dd, J = 0.8, 9.2 Hz, 1H), 7.75 (dd, J = 1.7, 9.2 Hz, 1H), 7.29-7.24 (m, 3H), 7.14-7.12 (m, 2H), 7.01-6.99 (m, 2H), 5.18 (s, 2H), 3.96-3.91 (m, 1H), 2.58 (d, J = 7.7 Hz, 2H), 2.06 (s, 6H), 1.75 (d, J = 2.4 Hz, 3H).

Crystalline form of compound 4 and X-ray structure characterization. (3S)-3-[4-[[2-(2,6-Dimethylphenyl)-[l,2,4]triazolo[l,5-a]pyridin-6- yl]methoxy]phenyl]hex-4-ynoic acid **4** was be prepared as a crystalline anhydrous form by dissolving (3S)-3-[4-[[2-(2,6-Dimethylphenyl)-[l,2,4] triazolo[l,5-a]pyridin-6-yl]methoxy]phenyl]hex-4-ynoic acid (580 mg, 132 mmol) in EtOH (1.2 mL) with stirring at 80 °C for 10

min. The solution was filtered and cooled to 70 °C, and treated with seeds. The mixture was cooled slowly to ambient temperature while stirring overnight. The resulting solid was triturated with heptane and the solids are recovered by vacuum filtration and dried under vacuum at 60 °C to give the crystalline title product (438 mg, 75.5%). The XRD patterns of crystalline solids were obtained on a Bruker D4 Endeavor Xray powder diffractometer, equipped with a CuKa source (λ = 1.54060 A) and a Vantec detector, operating at 35 kV and 50 mA. The sample was scanned between 4 and 40° with a step size of 0.0087° and a scan rate of 0.5 seconds/step, and with 0.6 mm divergence, 5.28mm fixed anti-scatter, and 9.5 mm detector slits. The dry powder was packed on a quartz sample holder and a smooth surface was obtained using a glass slide. Confirmation of a crystal form may be made based on any unique combination of distinguishing peaks (in units of ° 20), typically the more prominent peaks. The crystal form diffraction patterns collected at ambient temperature and relative humidity were adjusted based on NIST 675 standard peaks at 8.85 and 26.77 degrees 2-theta. A prepared sample of (3S)-3-[4-[[2-(2,6-Dimethylphenyl)-[l,2,4]triazolo[l,5-a]pyridin-6-yl]methoxy]phenyl]hex-4-ynoic acid **4** was characterized by an XRD pattern using CuKa radiation as having diffraction peaks (2-theta values). The pattern contains a peak at 17.55 in combination with one or more of the peaks selected from the group consisting of 5.82, 10.78, 19.65, 21.31, and 24.33 with a tolerance for the diffraction angles of 0.2 degrees.

Biological Methods. All *in vitro* assays including, binding, calcium flux, β-arrestin agonist and peroxisome proliferator-activated receptor (PPAR) α, δ, γ assays were described previously in detail[26]. The use of animals was in accordance with international guidelines (NIH 85-23) and was approved by the local animal ethics committee at Lilly Research Laboratories.

Glucose Dependent Insulin Secretion (GDIS) in Rat Islet: GDIS assays were performed in primary islets. Pancreatic islets of Langerhans were isolated from male SD (Sprague Dawley) rats by collagenase digestion and Histopaque density gradient separation. The islets were cultured overnight in RPMI-1640 medium with GlutaMAXn to facilitate recovery from the isolation process. Insulin secretion was determined using 90 min incubation in EBSS (Earle's Balances Salt Solution) buffer in a 48-well plate. Islets were first preincubated in EBSS with 2.8 mM glucose for 60 min then transferred to a 48-well plate (four islets/well) containing 150 μL 2.8 mM glucose, and incubated with 150 μL of EBSS with 2.8 or 11.2 mM glucose in the presence or absence of test compounds for 90 min. The buffer was removed from the wells at the end of the incubation period and assayed for insulin levels using a rat insulin ELISA kit (Mercodia).

Oral Glucose Tolerance Test (OGTT) in Zucker fa/fa Rats: OGTTs were performed in Male Zucker fa/fa rats (10 weeks of age), a rodent model of insulin resistance, after 1 and 21 days of oral administered. Compounds were administered orally at various doses to provide a dose response efficacy curve. Compound **1** served as the positive control and reference standard for the study. OGTTs were performed one hour after compound administration with blood samples taken for determination of glucose and insulin levels at 0, 10, 20, 40, and 60 minutes post glucose administration (2g/kg).

ASSOCIATED CONTENT

Supporting information

Molecular formula strings and the associated biochemical and biological data as a CSV file. This material is available free of charge via the Internet at http://pubs.acs.org.

AUTHOR INFORMAITON

Corresponding Author

*Phone: 317-797-4751. E-mail: hamdouchi_chafiq@lilly.com or chafiq.hamdouchi@gmail.com

Author Contributions

The manuscript was written through contribution of all authors. All authors have given approval to the final version of the manuscript.

Notes

The authors declare no competing financial interest.

ACKNOWLEDGEMENT

We thank the GPR40 team at both Lilly and Jubilant for their dedicated efforts. We also thank Dr. Ruth Gimeno, Dr. Guoxin Zhu, Dr. Thomas Hardy and Dr, Timothy Grese for helpful discussions.

ABBREVIATIONS USED

GPR40, G protein-coupled receptor 40; FFAR1, Free Fatty Acid Receptor 1; GDIS, glucose dependent insulin secretion; PK, pharmacokinetics; AUC, area under curve; CL, plasma clearance; T2DM, type 2 diabetes mellitus; SAR, structure activity relationship; PPAR, peroxisome proliferator activator receptor; FLIPR, fluorescence imaging plate reader.

REFERENCES

(1) World Health Organization. *Global report on diabetes*. http://apps.who.int/iris/bitstream/10665/204871/1/9789241565257_eng.pdf (accessed May 26, 2016).

(2) Briscoe, C. P.; Peat, A. J.; McKeown, S. C.; Corbett, D. F.; Goetz, A. S.; Littleton, T. R.; McCoy, D. C.; Kenakin, T. P.; Andrews, J. L.; Ammala, C.; Fornwald, J. A.; Ignar, D. M.; Jenkinson, S. Pharmacological regulation of insulin secretion in MIN6 cells through the fatty acid receptor GPR40: identification of agonist and antagonist small molecules. *Br. J. Pharmacol.* **2006,** *148*, 619-628.

(3) Fujiwara, K.; Maekawa, F.; Yada, T. Oleic acid interacts with GPR40 to induce Ca2+ signaling in rat islet beta-cells: mediation by PLC and L-type Ca2+ channel and link to insulin release. *Am. J. Physiol. Endocrinol. Metab.* **2005,** *289*, E670-677.

(4) Nagasumi, K.; Esaki, R.; Iwachidow, K.; Yasuhara, Y.; Ogi, K.; Tanaka, H.; Nakata, M.; Yano, T.; Shimakawa, K.; Taketomi, S.; Takeuchi, K.; Odaka, H.; Kaisho, Y. Overexpression of GPR40 in pancreatic beta-cells augments glucose-stimulated insulin secretion and improves glucose tolerance in normal and diabetic mice. *Diabetes* **2009,** *58*, 1067-1076.

(5) Schnell, S.; Schaefer, M.; Schofl, C. Free fatty acids increase cytosolic free calcium and stimulate insulin secretion from beta-cells through activation of GPR40. *Mol. Cell. Endocrinol.* **2007,** *263*, 173-180.

(6) Shapiro, H.; Shachar, S.; Sekler, I.; Hershfinkel, M.; Walker, M. D. Role of GPR40 in fatty acid action on the beta cell line INS-1E. *Biochem. Biophys. Res. Commun.* **2005,** *335*, 97-104.

(7) Briscoe, C. P.; Tadayyon, M.; Andrews, J. L.; Benson, W. G.; Chambers, J. K.; Eilert, M. M.; Ellis, C.; Elshourbagy, N. A.; Goetz, A. S.; Minnick, D. T.; Murdock, P. R.; Sauls, H. R., Jr.; Shabon, U.; Spinage, L. D.; Strum, J. C.; Szekeres, P. G.; Tan, K. B.; Way, J. M.; Ignar, D. M.; Wilson, S.; Muir, A. I. The orphan G protein-coupled receptor GPR40 is activated by medium and long chain fatty acids. *J. Biol. Chem.* **2003,** *278*, 11303-11311.

(8) Itoh, Y.; Kawamata, Y.; Harada, M.; Kobayashi, M.; Fujii, R.; Fukusumi, S.; Ogi, K.; Hosoya, M.; Tanaka, Y.; Uejima, H.; Tanaka, H.; Maruyama, M.; Satoh, R.; Okubo, S.; Kizawa, H.; Komatsu, H.; Matsumura, F.; Noguchi, Y.; Shinohara, T.; Hinuma, S.; Fujisawa, Y.; Fujino, M. Free fatty acids regulate insulin secretion from pancreatic beta cells through GPR40. *Nature* **2003,** *422*, 173-176.

(9) Mancini, A.; Bertrand, G.; Vivot, K.; Carpentier, E.; Tremblay, C.; Ghislain, J.; Bouvier, M.; Poitout, V. beta-arrestin recruitment and biased agonism at free fatty acid receptor 1. *J Biol Chem* **2015,** *290*, 21131–21140.

(10) Edfalk, S.; Steneberg, P.; Edlund, H. Gpr40 is expressed in enteroendocrine cells and mediates free fatty acid stimulation of incretin secretion. *Diabetes* **2008,** *57*, 2280-2287.

(11) Hira, T.; Mochida, T.; Miyashita, K.; Hara, H. GLP-1 secretion is enhanced directly in the ileum but indirectly in the duodenum by a newly identified potent stimulator, zein hydrolysate, in rats. *Am. J. Physiol. Gastrointest. Liver Physiol.* **2009,** *297*, G663-671.

(12) Prentki, M.; Tornheim, K.; Corkey, B. E. Signal transduction mechanisms in nutrient-induced insulin secretion. *Diabetologia* **1997,** *40 Suppl 2*, S32-41.

(13) Xiong, Y.; Swaminath, G.; Cao, Q.; Yang, L.; Guo, Q.; Salomonis, H.; Lu, J.; Houze, J. B.; Dransfield, P. J.; Wang, Y.; Liu, J.; Wong, S.; Schwandner, R.; Steger, F.; Baribault, H.; Liu, L.; Coberly, S.; Miao, L.; Zhang, J.; Lin, D. C. H.; Schwarz, M. Activation of FFA1 mediates GLP-1 secretion in mice. Evidence for allosterism at FFA1. *Mol. Cell. Endocrinol.* **2013,** *369*, 119-129.

(14) Brown, S. P.; Dransfield, P. J.; Vimolratana, M.; Jiao, X.; Zhu, L.; Pattaropong, V.; Sun, Y.; Liu, J.; Luo, J.; Zhang, J.; Wong, S.; Zhuang, R.; Guo, Q.; Li, F.; Medina, J. C.; Swaminath, G.; Lin, D. C.; Houze,

J. B. Discovery of AM-1638: a potent and orally bioavailable GPR40/FFA1 full agonist. *ACS Med. Chem. Lett.* **2012,** *3*, 726-730.

(15) Burant, C. F.; Viswanathan, P.; Marcinak, J.; Cao, C.; Vakilynejad, M.; Xie, B.; Leifke, E. TAK-875 versus placebo or glimepiride in type 2 diabetes mellitus: a phase 2, randomised, double-blind, placebo-controlled trial. *Lancet* **2012,** *379*, 1403-1411.

(16) Christiansen, E.; Due-Hansen, M. E.; Urban, C.; Grundmann, M.; Schmidt, J.; Hansen, S. V.; Hudson, B. D.; Zaibi, M.; Markussen, S. B.; Hagesaether, E.; Milligan, G.; Cawthorne, M. A.; Kostenis, E.; Kassack, M. U.; Ulven, T. Discovery of a potent and selective free fatty acid receptor 1 agonist with low lipophilicity and high oral bioavailability. *J. Med Chem* **2013,** *56*, 982-992.

(17) Christiansen, E.; Due-Hansen, M. E.; Urban, C.; Grundmann, M.; Schroder, R.; Hudson, B. D.; Milligan, G.; Cawthorne, M. A.; Kostenis, E.; Kassack, M. U.; Ulven, T. Free fatty acid receptor 1 (FFA1/GPR40) agonists: mesylpropoxy appendage lowers lipophilicity and improves ADME properties. *J. Med Chem* **2012,** *55*, 6624-6628.

(18) Christiansen, E.; Urban, C.; Merten, N.; Liebscher, K.; Karlsen, K. K.; Hamacher, A.; Spinrath, A.; Bond, A. D.; Drewke, C.; Ullrich, S.; Kassack, M. U.; Kostenis, E.; Ulven, T. Discovery of potent and selective agonists for the free fatty acid receptor 1 (FFA(1)/GPR40), a potential target for the treatment of type II diabetes. *J. Med Chem* **2008,** *51*, 7061-7064.

(19) Kaku, K.; Araki, T.; Yoshinaka, R. Randomized, double-blind, dose-ranging study of TAK-875, a novel GPR40 agonist, in Japanese patients with inadequately controlled type 2 diabetes. *Diabetes Care* **2013,** *36*, 245-250.

(20) Lin, D. C.; Zhang, J.; Zhuang, R.; Li, F.; Nguyen, K.; Chen, M.; Tran, T.; Lopez, E.; Lu, J. Y.; Li, X. N.; Tang, L.; Tonn, G. R.; Swaminath, G.; Reagan, J. D.; Chen, J. L.; Tian, H.; Lin, Y. J.; Houze, J. B.; Luo, J. AMG 837: a novel GPR40/FFA1 agonist that enhances insulin secretion and lowers glucose levels in rodents. *PLoS ONE* **2011,** *6*, e27270.

(21) Naik, H.; Vakilynejad, M.; Wu, J.; Viswanathan, P.; Dote, N.; Higuchi, T.; Leifke, E. Safety, tolerability, pharmacokinetics, and pharmacodynamic properties of the GPR40 agonist TAK-875: results from a double-blind, placebo-controlled single oral dose rising study in healthy volunteers. *J. Clin. Pharmacol.* **2012,** *52*, 1007-1016.

(22) Negoro, N.; Sasaki, S.; Mikami, S.; Ito, M.; Suzuki, M.; Tsujihata, Y.; Ito, R.; Harada, A.; Takeuchi, K.; Suzuki, N.; Miyazaki, J.; Santou, T.; Odani, T.; Kanzaki, N.; Funami, M.; Tanaka, T.; Kogame, A.; Matsunaga, S.; Yasuma, T.; Momose, Y. Discovery of TAK-875: a potent, selective, and orally bioavailable GPR40 agonist. *ACS Med. Chem. Lett.* **2010,** *1*, 290-294.

(23) Poitout, V.; Lin, D. C. Modulating GPR40: therapeutic promise and potential in diabetes. *Drug Discovery Today* **2013,** *18*, 1301-1308.

(24) Sasaki, S.; Kitamura, S.; Negoro, N.; Suzuki, M.; Tsujihata, Y.; Suzuki, N.; Santou, T.; Kanzaki, N.; Harada, M.; Tanaka, Y.; Kobayashi, M.; Tada, N.; Funami, M.; Tanaka, T.; Yamamoto, Y.; Fukatsu, K.; Yasuma, T.; Momose, Y. Design, synthesis, and biological activity of potent and orally available G protein-coupled receptor 40 agonists. *J. Med. Chem.* **2011,** *54*, 1365-1378.

(25) Shimada, T.; Ueno, H.; Tsutsumi, K.; Aoyagi, K.; Manabe, T.; Sasaki, K.; Kato, H. Spiro-Ring Compound and Use Thereof for Medical Purposes. PCT Int. Appl. WO 2009054479 A1, April 30, 2009.

(26) Hamdouchi, C.; Kahl, S. D.; Patel Lewis, A.; Cardona, G. R.; Zink, R. W.; Chen, K.; Eessalu, T. E.; Ficorilli, J. V.; Marcelo, M. C.; Otto, K. A.; Wilbur, K. L.; Lineswala, J. P.; Piper, J. L.; Coffey, D. S.; Sweetana, S. A.; Haas, J. V.; Brooks, D. A.; Pratt, E. J.; Belin, R. M.; Deeg, M. A.; Ma, X.; Cannady, E. A.; Johnson, J. T.; Yumibe, N. P.; Chen, Q.; Maiti, P.; Montrose-Rafizadeh, C.; Chen, Y.; Reifel Miller, A. The discovery, preclinical, and early clinical cevelopment of potent and selective G protein-coupled receptor 40 (GPR40) agonists for the treatment of type 2 diabetes mellitus. *J. Med. Chem.* **2016,** *59*, 10891-10916.

(27) Mendiola, J.; Rincón, J. A.; Mateos, C.; Soriano, J. F.; de Frutos, Ó.; Niemeier, J. K.; Davis, E. M. Preparation, use, and safety of O-mesitylenesulfonylhydroxylamine. *Org. Process Res. Dev.* **2009,** *13*, 263-267.

(28) Smith, D. A.; Di, L.; Kerns, E. H. The effect of plasma protein binding on in vivo efficacy: misconceptions in drug discovery. *Nat. Rev. Drug Discov.* **2010,** *9*, 929-939.

(29) Hamdouchi, C. Preparation of Novel Triazolo-Pyridine Compounds for Treating Diabetes. PCT Int. Appl. WO 2015088868 A1, June 18, 2015.

Scheme 1. Synthesis of [1,2,4]triazolo[1,5–a]pyridine acid derivatives (route A)[a]

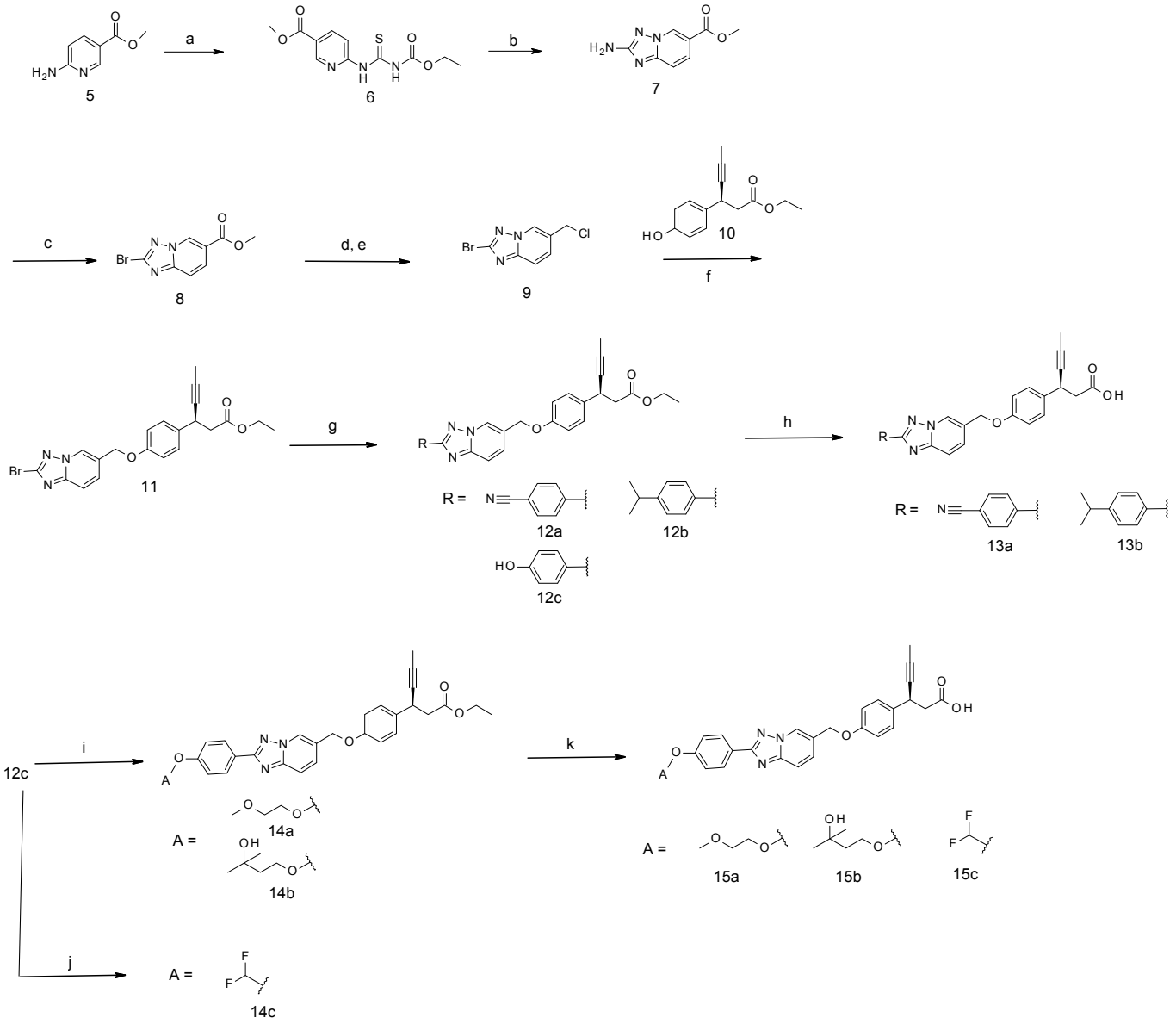

[a]Reagents and conditions: (a) Ethyl N-(thiomethylene)carbamate, methyl 6 aminopyridine-3-carboxyalte, 1:4 dioxane, rt, 7 h, 88%; (b) Hydroxylamine hydrochloride, DIPEA, methanol, rt, 40 hr, 76%; (c) $CuBr_2$, t-BuCN, 60 ^oC, 1h, 48%; (d) DCM, DIBAL-H, -78 ^oC, 1h, 58%; (e) $SOCl_2$, 0 ^oC to rt,1h, 100% (used without purification for the next step); (f) $CsCO_3$, rt, 14h, 80%; (g) 4-substituted phenylboronic acids, K_2CO_3-2M, $Pd(PPh_3)_2Cl_2$, microwave 100 ^oC, 4 to 12 h, 57-74%; (h) $KOSiMe_3$, THF, 2h, rt, or NaOH-5N, EtOH, 80 ^oC, 30min; (i) Cs_2CO_3, ACN, rt, 2 to 12 h, 64 to 100%; (j) sodium chlorodifluroacetate, DMF, Cs_2CO_3, 80 ^oC, 4h, 56%; (k) 5 N NaOH, ethanol, rt to 80 ^oC, 30 min to 16 h, 60-90%.

Scheme 2. Synthesis of [1,2,4]triazolo[1,5–a]pyridine acid derivatives (route B)[a]

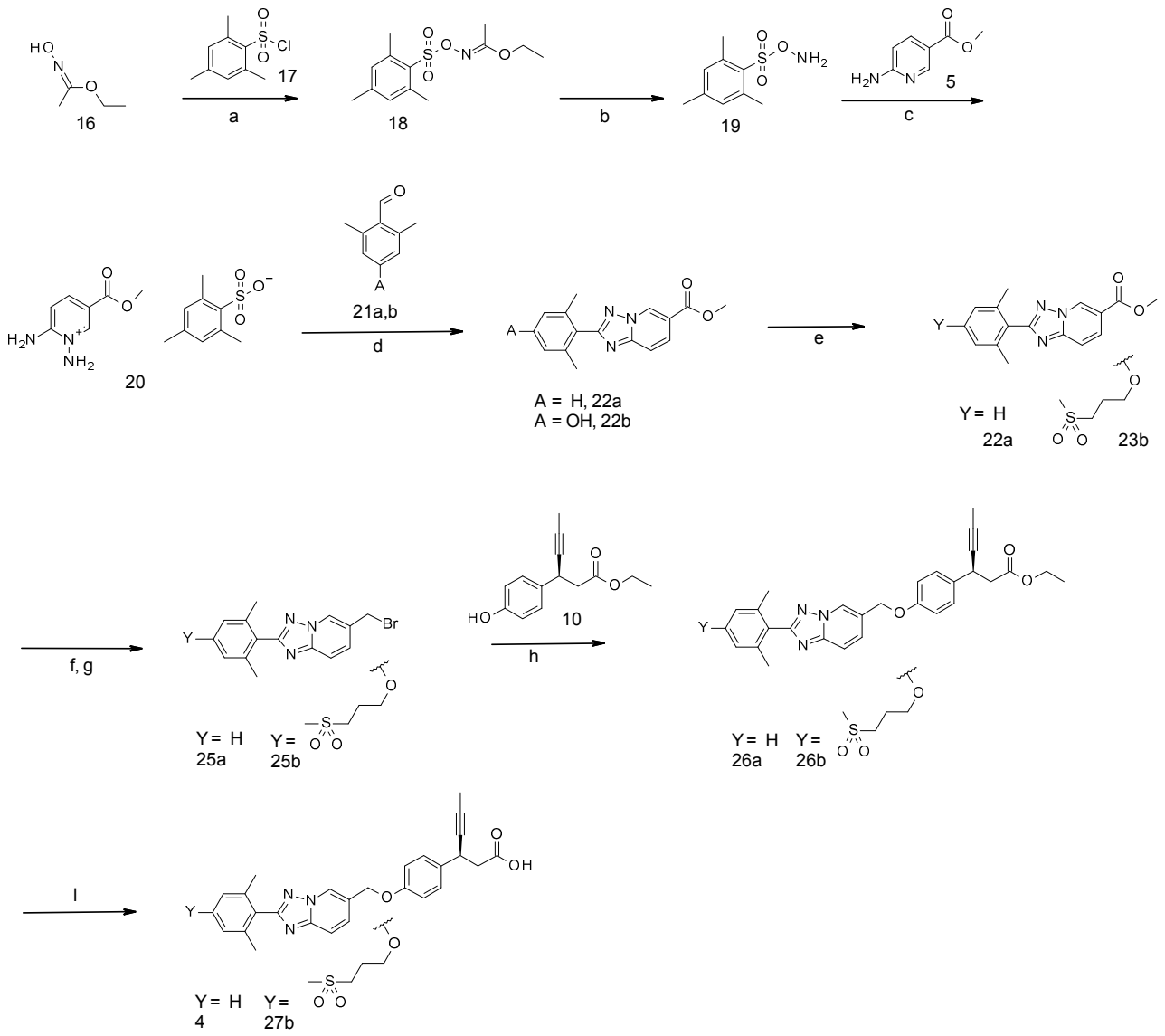

[a]Reagents and conditions: (a) DMF, TEA, rt, 16 h, 64%; (b) $HClO_4$, 0 °C to rt, 1 h, 100% (used without purification for the next step); (c) DCM, rt, 16 h, 41%; (d) TEA, methanol , rt 18-48 h, 18-40%; (e) K_2CO_3, ACN, 100 °C, 16 h, 70%; (f) DIBAL-H DCM, 0 °C to rt, 2 h, 57%; (g) PBr_3, DCM, rt, 2 h, 76%; (h) $CsCO_3$, DMF, rt, 16 h, 57%; (i) NaOH, EtOH/H_2O, rt, 16 h, 93 and 55%.

Scheme 3. Process chemistry synthesis of [1,2,4]triazolo[1,5–a]pyridine acid 4 on 36 kg scale[a]

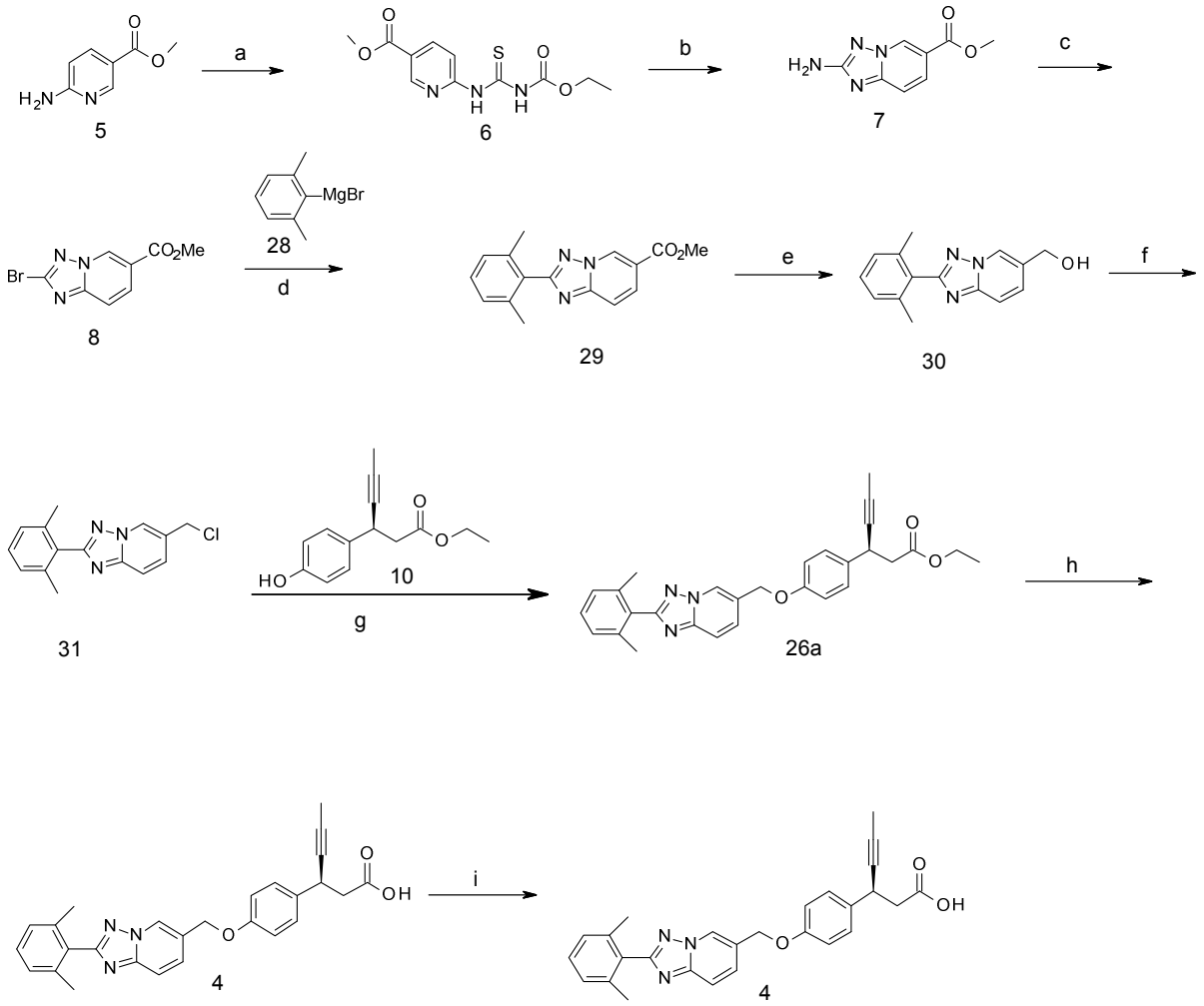

[a]Reagents and conditions: (a) Ethyl N-(thiomethylene)carbamate, methyl 6 aminopyridine-3-carboxyalte, THF, 45 to 50 °C, 15 h, 91%; (b) Hydroxylamine hydrochloride, DIPEA, ethanol, 55 to 60 °C, 8 hr, 96%; (c) $CuBr_2$, ACN/t-BuCN, 45 to 50 °C, 1h, 63%; (d) THF, $ZnCl_2$, $Pd(Ph_3)_4$, 50-55 °C; (e) DCM, toluene, DIBAL-H, -10 °C to -15 °C, 80% over two steps; (f) $SOCl_2$, THF, 20 to 30°C, 88%; (g) DMF, K_2CO_3, 35-45 °C; (h) NaOH, EtOH, 25 °C; 88% over two steps; (i) EtOH, seed with compound **4**; n-heptane; 91%.

Table 1. *In vitro* activities of triazolopyridine phenyl propanoic acids

			Human GPR40 Binding[a]	Human GPR40 β-arrestin 1% FBS[b]		Rat GPR40 β-arrestin 1% FBS[c]		Human GPR40 Calcium[d]		Calculated properties[e]
LSN	Cmpd	R	Ki, nM (SEM, n)	EC_{50}, nM (SEM, n)	% Stim Max (SEM, n)	EC_{50}, nM (SEM, n)	% Stim Max (SEM, n)	EC_{50}, nM (SEM, n)	% Stim Max (SEM, n)	PSA
3104607	4		15 (4, n=4)	108 (34, n=23)	124 (6, n=23)	14 (5, n=9)	130 (6, n=9)	11 (7, n=3)	54 (10, n=3)	77
3199272	15a		102 (12, n=3)	681 (132, n=8)	121 (6, n=8)	562 (273, n=5)	133 (14, n=5)	16 (13, n=3)	74 (5, n=3)	95
3199271	13b		32 (11.5, n=3)	67 (15, n=8)	154 (8, n=8)	30 (8, n=5)	123 (6, n=5)	2 (1, n=3)	65 (6, n=3)	77
3199270	15b		37 (8, n=3)	301 (116, n=8)	132 (14, n=8)	68 (33, n=5)	121 (13, n=5)	72 (3, n=3)	89 (2, n=3)	106
3156275	27b		63 (5, n=3)	1490 (809, n=6)	114 (10, n=6)	95 (31, n=5)	140 (5, n=5)	117 (38, n=3)	71 (1, n=3)	129
3203801	13a		35 (6, n=3)	443 (86, n=8)	124 (6, n=8)	216 (62, n=5)	125 (7, n=5)	9 (4, n=4)	65 (8, n=4)	101
3199273	15c		60 (17, n=4)	166 (47, n=8)	127 (8, n=8)	98 (54, n=5)	142 (12, n=5)	1.0 (0.3, n=3)	64 (1, n=3)	86

[a]Competitive inhibition with human GPR40 membranes.[26] [b,c]β-arrestin recruitment with human and rat GPR40 in the presence of 1% fetal bovine serum (FBS). [d]Calcium flux with human GPR40; the percent of stimulation is relative to the 100 μM of the natural ligand, linoleic acid, response. [e]PSA values were computed using Chemaxon software.

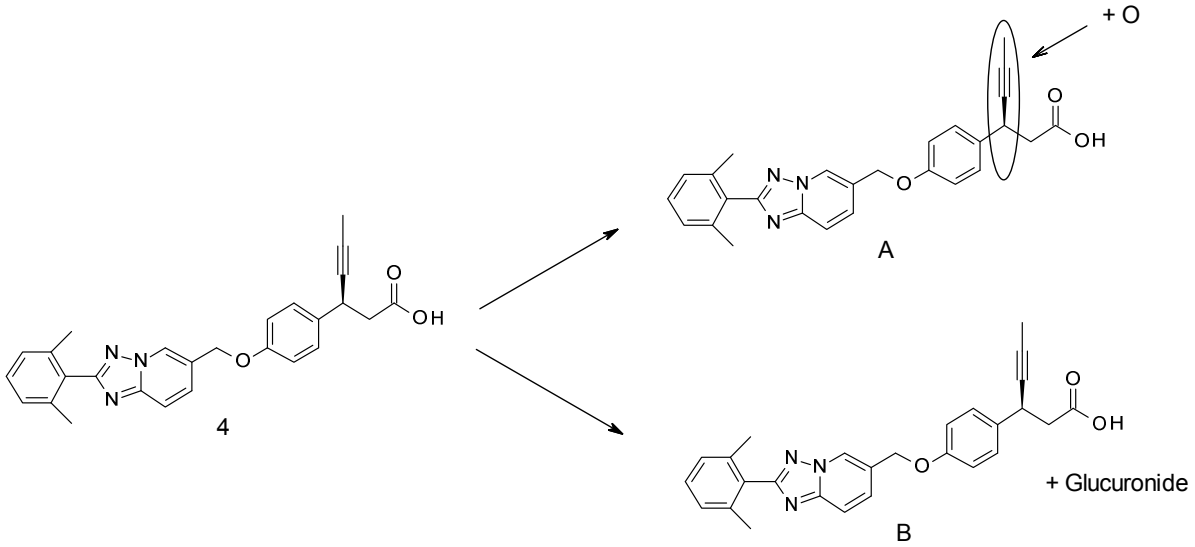

Figure 1. Major Metabolic Pathways of **4**

Table 2. Mean Pharmacokinetic Parameters of 4 in rats and dogs

Rat					
Dose (mg/kg)	1	1	10	100	500
Route	IV	Oral	Oral	Oral	Oral
AUC $_{0-24\ h}$ (ng x hr/mL)	12726 ± 2086	11672 ± 2942	215000 ± 77100	2870000 ± 281000	4790000 ± 3560000
Co or Cmax (ng/mL)	4337 ± 1144	3380 ± 782	23700 ± 2290	208000 ± 10400	281000 ± 191000
Tmax (hours)		0.25 ± 0.0	4.0 ± 0.0	5.3 ± 2.3	6.7 ± 2.3
CL mL/min/kg	1.32 ± 0.20				
Vdss (L/kg)	0.33 ± 0.02				
T1/2 (hours)	3.98 ± 0.14	4.68 ± 0.86	Not Calculated	Not Calculated	Not Calculated
Bioavailability (%)		93	Not Calculated	Not Calculated	Not Calculated

Dog					
Dose mg/kg	1	3	30[a]	100[a]	300[a]
Route	IV	Oral	Oral	Oral	Oral
AUC 0−24 h ng x hr/mL	27300 ± 3830	52800 ± 26100	120000	3320000	4010000
Co or Cmax ng/mL	8240 ± 399	9900 ± 4730	126000	260000	277000
Tmax hours		0.67 ± 0.29	2	3	6
CL mL/min/kg	0.601 ± 0.094				
Vdss L/kg	0.27 ± 0.08				
T1/2 hours	6.53 ± 1.92	5.49 ± 0.83	Not Calculated	Not Calculated	Not Calculated
Bioavailability%		83	Not Calculated	Not Calculated	Not Calculated

[a]N = 2

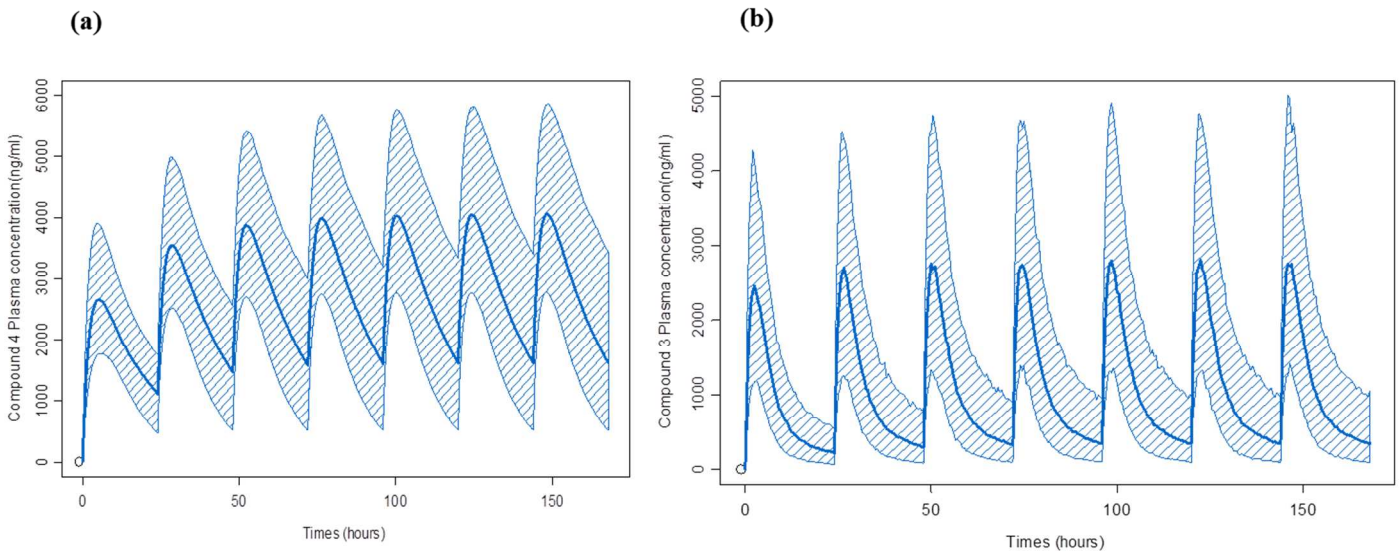

Figure 2. Comparison of human pharmacokinetics: (a) predicted human PK profile for compound **4** simulated based on projected PK parameters; (b) human PK profile for compound **3** simulated using PK parameters from the SAD study.

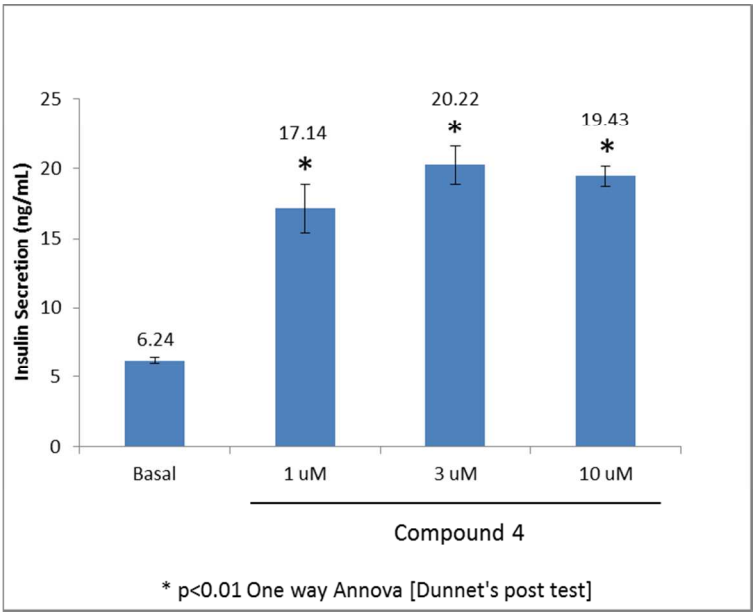

Figure 3. Stimulation of insulin secretion by **4** in rat islets.

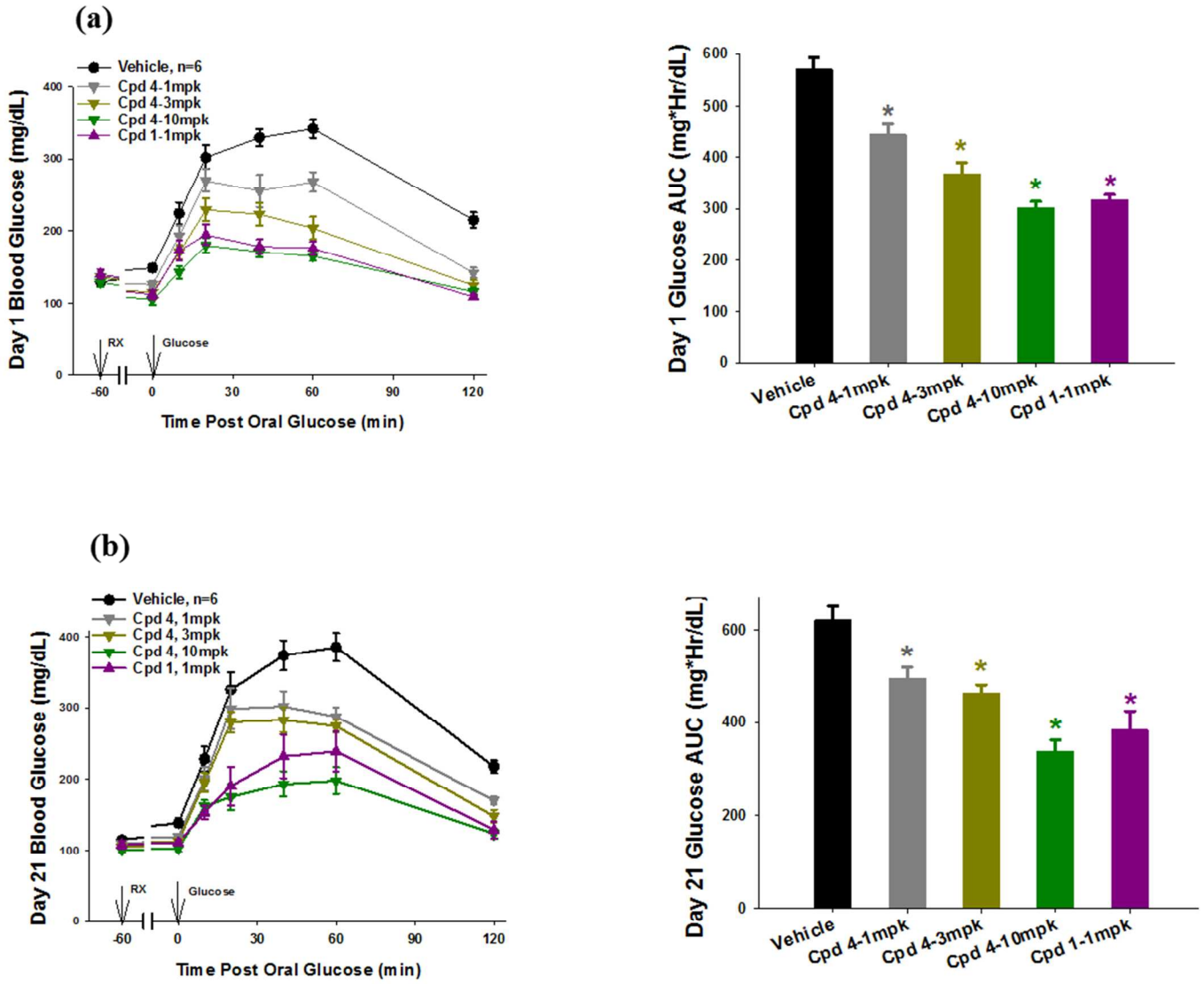

Figure 4. Glucose levels during OGTTs performed on days 1(a) and 21(b) in Zucker fa/fa rats. OGTTs were performed 1h post compound administration with blood samples taken for determination of glucose levels at 0, 10, 20, 40, 60 and 120 min post glucose administration (2 g/kg)

Table 3. Drug metabolism and developability assessment of GPR40 agonists

Cmpd		1 (LY2881835)	2 (LY2922083)	3 (LY2922470)	4 (LY3104607)
Structure		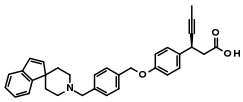	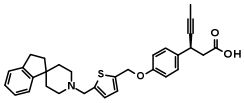	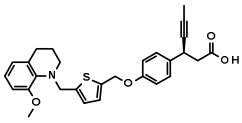	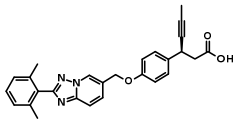
logP[a]	measured	4.9	5.0	5.2	4.8
pKa[b]	measured	4.1 and 8.1	3.4 and 7.9	3.4 and 6.0	4.3
PSA[c]	calculated	50	50	59	77
Metabolite identification[d]	mouse, rat, dog	O-dealkylation, oxidation and glucuronidation	N-dealkylation, oxidation and glucuronidation	glucuronidation and desmethylation	glucuronidation
Metabolic stability (%metabolized)[e]	mouse	79 (33, n=3)	98 (2, n=2)	38 (6, n=2)	7 (6, n=3)
	rat	64 (56, n=3)	98 (2, n=2)	62 (3, n=2)	10 (11, n=4)
	dog	65 (19, n=3)	93 (6, n=2)	18 (1, n=2)	5 (5, n=3)
	human	38 (20, n=3)	44 (8, n=2)	24 (4, n=2)	5 (6, n=4)
Microsomal CL Kdep (hr^{-1})[f]	human	0.033 ± 0.002	0.109 ± 0.001	0.0048 + 0.0004	< 0.0009
Hepatocyte CL Kdep (hr^{-1})[g]	human	0.28 ± 0.03	0.23 ± 0.04	0.17 ± 0.05	0.099 + 0.019
Clearance CL (L/h)[h]	human	11 (found)	31 – 43 (found)	11 - 14 (found)	1, 90% PI: (0.5, 1.6) (predicted)
Vd (L)[i]	human	111 (found)	443-885 (found)	244-358 (found)	19, 90% PI: (16, 22) (predicted)
Predicted Exposure[j]	human	Large peak to trough ratio	Large peak to trough ratio	Large peak to trough ratio	Small peak to trough ratio
Solubility[k]	Aq. pH 7.4 uM	61 - 80	89 - 70	>100	>100
DSC[l]	Celcius	153	167	117	151
cPeff[m]	$x10^{-4}$ cm/sec	6	5	6	5.2
H cDabs Fasted[n]	MiMBa	166	127	845	593
H cDabs Fed[o]	MiMBa	467	149	797	919
Human GPR40 binding[p]	Ki nM	4.7	8.2	27	15
Human GPR40 Calcium[q]	EC_{50} nM (% Eff.)	9.1 (62%)	8.0 (50%)	3.0 (51%)	11 (54%)
OGTT in Zucker *fa/fa* rats[r]	ED_{90} mg/kg	1	14.2	3.3	5

[a,b]logP and pKa values were measured.[c]PSA values were computed using Chemaxon software. [d]Metabolite identfication in mouse, rat, and dog hepatocytes. [e]Metabolic stability; % metabolized following a 30 min incubation in mouse or human microsomes. [f]Microsomal human microsomes. [g]Hepatocyte clearance in human hepatocytes. [l]Differential scanning calorimetry. [h]Human clearance determined clinically for compounds **1**, **2** and **3** in type two diabetes patients and predicted for compound **4** using allometric scaling. [i]Human volume of distribution determined clinically for compounds **1**, **2** and **3** in type two diabetes patients and predicted for compound **4** using allometric scaling. [j]Predicted exposure based on predicted human CL and Vd. [k]Measured solubility at pH 7.4. [l]Differential scanning calorimetry. [m]Calculated human passive permeability. [n,o]Calculated human absorbable dose, fasted state. [p]Competitive inhibition with human GPR40

membranes. [q]Calcium flux with human GPR40. [r]Effect of GPR40 agonists during an OGTT in Zucker *fa/fa* rats: glucose lowering ED_{90} on day 21.

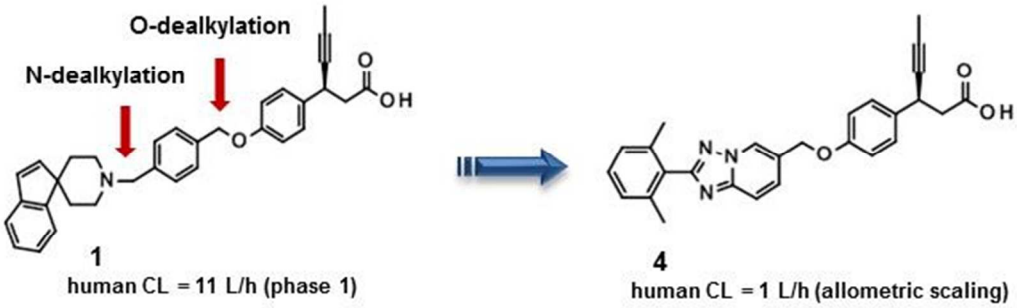

Table of Contents Graphic